

**Figure 3.** Representative pictures of cardiac histology. Row A, representative images of whole-heart cross section obtained by microscopic analysis (hematoxylin-eosin stain). LV wall thickness was markedly decreased in celiprolol ( $100 \text{ mg} \cdot \text{kg}^{-1} \cdot \text{d}^{-1}$ )-treated compared with TAC mice. Row B, cardiac myocyte cross surface (hematoxylin-eosin stain; magnification  $\times 400$ ; scar =  $20 \mu\text{m}$ ). Row C, long-axis view of cardiac myocyte (hematoxylin-eosin stain,  $\times 200$ ). Myocardial fibrosis (row D) and perivascular fibrosis (row E) were stained with azan-Mallory stain ( $\times 100$ ).

hypothesized that celiprolol may inhibit cardiac remodeling via the NO signal pathway. To test this idea, we evaluated the effects of long-term treatment with celiprolol on cardiac hypertrophy and heart function in a murine model of ventricular pressure overload induced by transverse aortic constriction (TAC). We examined plasma NO levels, myocardial eNOS protein levels, and its phosphorylation. We also tried to

confirm whether celiprolol-induced attenuation of cardiac hypertrophy is blunted by  $N^G$ -nitro-L-arginine methyl ester (L-NAME). Moreover, to delineate the role of NO in cardiac hypertrophy and failure, we measured cardiac hypertrophy, pulmonary congestion and plasma NO levels in a time course and analyzed the correlation among them.

## Methods

### Cell Culture

Rat neonatal ventricular myocytes were isolated and cultured as we described previously.<sup>13</sup> Cardiomyocytes were exposed to either phenylephrine (PE) ( $10^{-4} \text{ mol/L}$ ), or isoproterenol ( $10^{-6} \text{ mol/L}$  or other concentrations) for 24 hours in the presence or absence of celiprolol (Nippon Shinyaku Co Ltd), and the extent of increase in [ $^3\text{H}$ ]leucine uptake was examined. To test whether the inhibitory effect of celiprolol on protein synthesis induced by PE was mediated via release of NO, we used L-NAME in an attempt to suppress this effect.

### TAC Model and Protocols

All procedures were in accordance with institutional guidelines for animal research. Mice (C57BL/6, male, 8 to 9 weeks old, weighing 19 to 23 g) were anesthetized with a mixture of xylazine (5 mg/kg) and ketamine (25 mg/kg, intraperitoneal injection). The TAC model was created as we described previously.<sup>14,15</sup>

We treated the mice with saline (TAC group) or celiprolol at  $100 \text{ mg} \cdot \text{kg}^{-1} \cdot \text{d}^{-1}$  (PO, Celi low group) and  $200 \text{ mg} \cdot \text{kg}^{-1} \cdot \text{d}^{-1}$  (PO, Celi high group). L-NAME at  $100 \text{ mg} \cdot \text{kg}^{-1} \cdot \text{d}^{-1}$  in drinking water and L-NAME plus celiprolol  $100 \text{ mg} \cdot \text{kg}^{-1} \cdot \text{d}^{-1}$  PO were also used. No difference was found among all the experimental groups in age and body weight before surgery. Two to 3 mice in each group were used to measure the transstenosis pressure gradient. Tail-cuff blood pressure and heart rate were measured (BP-98A, Softron). Mice were euthanized at different time points after TAC, and morphometric analysis was performed. Cell surface area and myocardial and perivascular fibrosis measurements were performed using 3 hearts in each group as described previously.<sup>15,16</sup>

### Echocardiographic Assessment

Transthoracic echocardiography was performed with a Sonos 4500 and a 15-6 L MHz transducer (Philips). Mice were lightly anesthetized with 2.5% Avertin (0.06 mL/10 g) and fixed. When they had recovered consciousness ( $\approx 10$  minutes), good 2D short-axis views of the left ventricle (LV) were obtained for guided M-mode measurements of the LV posterior wall thickness, LV end-diastolic diameter, and LV end-systolic diameter.

### NO Measurement

The plasma levels of nitrite and nitrate ( $\text{NO}_x$ ) were measured as previously described.<sup>17</sup> Cardiac myocardial protein level of eNOS, inducible NOS (iNOS), neuronal NOS (nNOS), and eNOS phosphorylated activity were checked by use of Western blot analy-

### Hemodynamic and Echocardiographic Results

Group	Body Weight, g	Transstenosis Gradient Pressure, mm Hg (n=2-3 in each group)	Heart Rate, bpm	Tail-Cuff Systolic Blood Pressure, mm Hg	LV End-Systolic Dimension, mm	LV End-Diastolic Dimension, mm	LV Diastolic Posterior Wall Thickness, mm
Sham (10)	$24 \pm 0.3^*$	$5 \pm 1$	$640 \pm 21$	$116 \pm 2.9^*$	$1.64 \pm 0.04^*$	$3.07 \pm 0.06^*$	$0.65 \pm 0.02^*$
TAC (8)	$22.6 \pm 0.5$	$55 \pm 5$	$647 \pm 11$	$100 \pm 3.7$	$2.32 \pm 0.24$	$3.37 \pm 0.17$	$1.01 \pm 0.06$
TAC+Celi (11)	$22.4 \pm 0.7$	$52 \pm 4$	$604 \pm 17^*$	$108 \pm 3.1$	$1.83 \pm 0.1^*$	$3.04 \pm 0.11^*$	$0.79 \pm 0.03^*$
TAC+L-NAME (6)	$21.2 \pm 0.6$	$50 \pm 3$	$652 \pm 11$	$108 \pm 3.5$	$2.30 \pm 0.21$	$3.31 \pm 0.20$	$0.99 \pm 0.05$
TAC+Celi+L-NAME (5)	$21.9 \pm 0.5$	$54 \pm 3$	$616 \pm 13^*$	$106 \pm 2.1$	$1.95 \pm 0.2$	$3.15 \pm 0.12$	$0.93 \pm 0.02$

TAC indicates transverse aortic constriction; Celi, celiprolol  $100 \text{ mg} \cdot \text{kg}^{-1} \cdot \text{d}^{-1}$  PO. The number of mice in each group is indicated in parentheses.

\* $P < 0.05$  vs TAC.

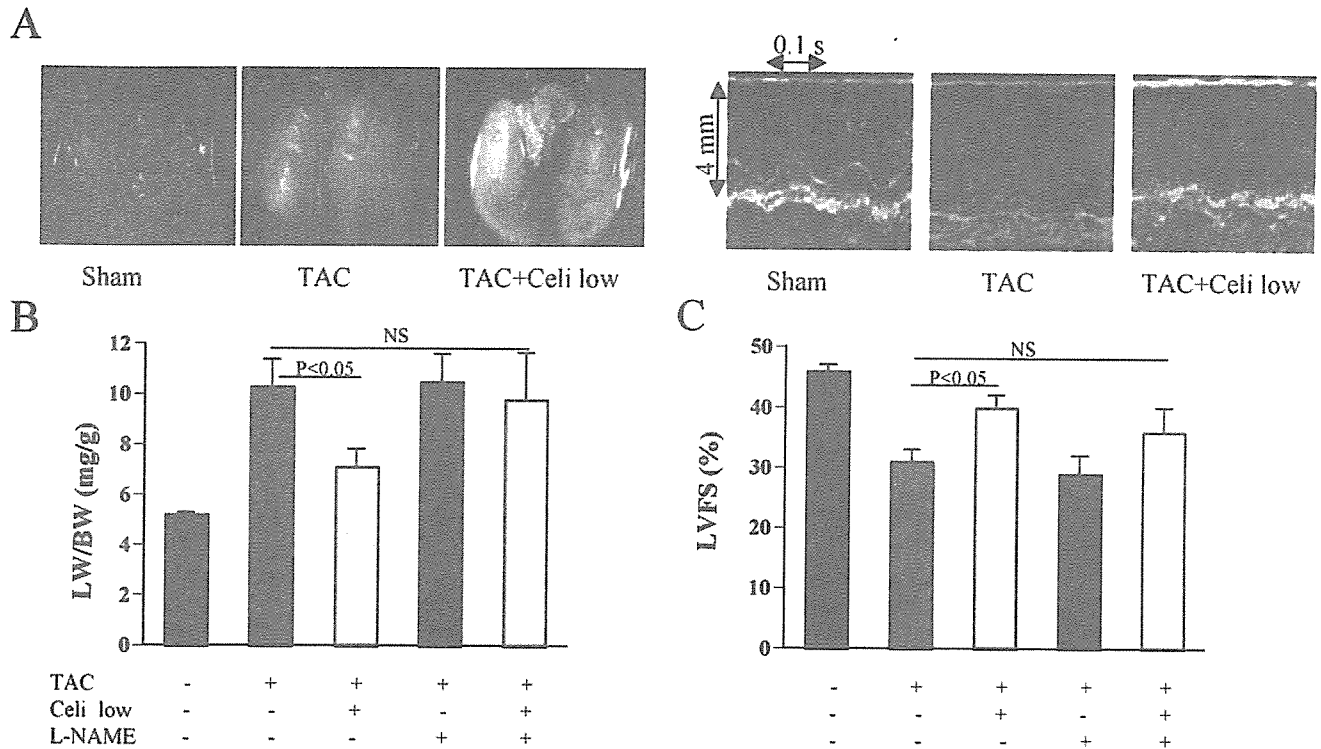


**Figure 4.** Celiprolol prevents heart failure induced by TAC. A, Representative images of echocardiography and macroscopic view of lungs in different groups. B, LW/BW ratio was decreased significantly in TAC mice treated with celiprolol  $100 \text{ mg} \cdot \text{kg}^{-1} \cdot \text{d}^{-1}$  in comparison with untreated TAC mice. L-NAME ( $100 \text{ mg} \cdot \text{kg}^{-1} \cdot \text{d}^{-1}$ ) alone did not affect heart function under conditions of LV pressure overload. However, it partially abolished antihypertrophic effect of celiprolol ( $100 \text{ mg} \cdot \text{kg}^{-1} \cdot \text{d}^{-1}$ ). C, LV fractional shortening was increased in response to celiprolol treatment. Number of mice in each group is same as described in Figure 3.

sis.<sup>16,18</sup> Expression of these proteins was detected by use of the diaminobenzidine method and quantified by densitometry.

### RNA Analysis

Assessment of the cardiac gene expression for natriuretic peptide precursor type B (BNP), protein inhibitor of NOS (PIN), and sarcoplasmic/endoplasmic reticulum calcium ATPase (SERCA2) was performed by real-time polymerase chain reaction (RT-PCR).<sup>19</sup> The Quantitect SYBR Green RT-PCR kit (Qiagen) was used to perform amplifications with the One-step protocol as described by the manufacturer.

### Statistical Analysis

For all statistical tests, multiple comparisons were performed by 1-way ANOVA with the Tukey-Kramer exact probability test. The least-squares method was used for linear correlation between selected variables. Data were reported as the mean  $\pm$  SEM. A value of  $P < 0.05$  was considered statistically significant.

## Results

### Celiprolol Inhibits Myocyte Protein Synthesis Induced by Either Isoproterenol or PE

Isoproterenol, a nonselective  $\beta$ -AR agonist, increased myocyte protein synthesis. The selective  $\beta_1$ -AR antagonist celiprolol suppressed the enhancement by 70% (Figure 1A), suggesting that it is predominantly  $\beta_1$ -ARs that mediate the isoproterenol-induced increase in protein content. As shown in Figure 1B, celiprolol also reduced the increase in protein synthesis stimulated by PE, indicative of an antihypertrophic effect independent of  $\beta_1$ -AR blockade. PE increased cell size, whereas celiprolol significantly suppressed the increase (Fig-

ure 1, C and D). The inhibition of eNOS by L-NAME partially abolished the antihypertrophic effect of celiprolol on the PE-induced increase in protein synthesis (Figure 1, B–D).

### Celiprolol Attenuates Pathological Cardiac Hypertrophy

Consistent with the results in vitro, low-dose celiprolol markedly attenuated cardiac hypertrophy 4 weeks after TAC (Figure 2, A and B). Histological examination also revealed that the extent of myocyte hypertrophy (Figure 3 A–C) was reduced and both myocardial and perivascular fibrosis were ameliorated in celiprolol-treated mice (Figure 2, C and D and Figure 3, D and E). The same results were achieved at a higher dose of celiprolol.

The results of hemodynamics and echocardiography measured just before the animals were killed are shown in the Table. Celiprolol reduced heart rate significantly but did not affect tail-cuff systolic blood pressure. The LV wall became thinner in celiprolol-treated mice than in TAC mice. Between the 2 celiprolol groups, no significant differences were noted in hemodynamic and echocardiographic findings, although there was a tendency for the LV cavity to be smaller, the LV wall to be thicker, and LV fractional shortening to be higher in mice treated with the higher dose (data not shown).

We recorded echocardiographs and hemodynamics for all mice before surgery and found no differences among the 6 groups (data not shown). The transstenosis pressure gradient measured in 2 to 3 mice in each group showed no significant difference (Table).

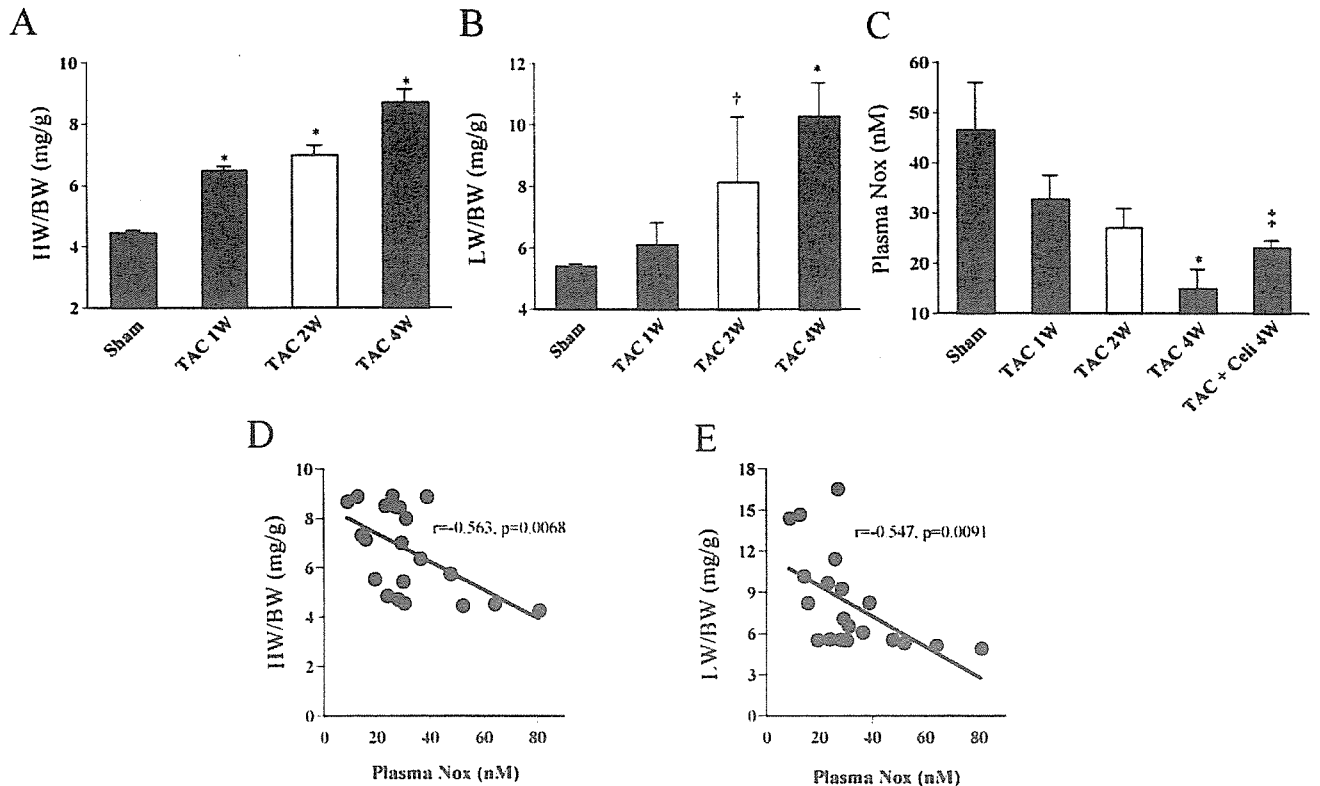


**Figure 5.** Time course of cardiac hypertrophy, pulmonary congestion, and NO production. HW/BW ratio (A) and LW/BW ratio (B) increased, plasma NO production (C) decreased time-dependently, and celiprolol ( $100 \text{ mg} \cdot \text{kg}^{-1} \cdot \text{d}^{-1}$ ) treatment increased NO production. Significant negative linear correlations were noted between HW/BW and plasma NO level (D) and LW/BW and plasma NO level (E). Numbers of mice in Sham, TAC 1 week (1w), TAC 2w, TAC 4w, and TAC+Celi groups are 6, 5, 5, 7, and 6, respectively. \* $P < 0.01$ , † $P < 0.05$  vs sham; ‡ $P < 0.01$  vs TAC 4w.

### L-NAME Partially Abolishes the Antihypertrophic Effect of Celiprolol

Treating TAC mice with celiprolol plus L-NAME decreased but did not completely abolish the antihypertrophic effect of celiprolol, whereas L-NAME alone did not further increase cardiac hypertrophy in the TAC mice (Figure 2, A–D).

### Celiprolol Prevents Transition to Heart Failure

TAC induced congestive heart failure, manifested by increases in lung weight and reductions in fractional shortening. Compared with values in sham-operated mice, the ratio of lung weight to body weight (LW/BW) increased by  $\approx 84\%$  in TAC mice but only by 27% in low-dose celiprolol-treated mice (Figure 4, A and B), respectively. LV fractional shortening was also significantly higher in celiprolol-treated mice than TAC mice (Figure 4C). The same results on heart function were achieved at the higher dose of celiprolol. Furthermore, L-NAME markedly counteracted these beneficial effects produced by celiprolol.

### NO Production Is Associated With Cardiac Hypertrophy and Heart Failure

To further clarify the role of NO in cardiac hypertrophy and heart failure, we evaluated the time course of cardiac hypertrophy, heart failure, and the plasma levels of  $\text{NO}_x$ . Heart weight-to-body weight ratio (HW/BW) and LW/BW were increased time-dependently from 1 to 4 weeks (Figure 5, A and B),

whereas plasma levels of  $\text{NO}_x$  were decreased time-dependently (Figure 5C). Significant negative linear correlations were found between HW/BW and plasma  $\text{NO}_x$  (Figure 5D) and between LW/BW and plasma  $\text{NO}_x$  (Figure 5E). We also noted that celiprolol treatment partially prevented the decrease of NO production in TAC mice (Figure 5C).

### Celiprolol Increases eNOS Protein and Its Activity

Myocardial protein levels of eNOS and its phosphorylation were decreased in TAC mice; celiprolol treatment increased eNOS and its phosphorylation significantly (Figure 6, A and B). We also tried to check the protein levels of iNOS and nNOS in myocardium with Western blot analysis and found that they were hardly detectable (data not shown), which is similar to previous reports.<sup>16,20</sup>

### Celiprolol Induces Altered Transcriptional Expression

As shown in Figure 7, quantitative real-time PCR demonstrated that celiprolol treatment decreased levels of the hypertrophic molecular marker BNP, downregulated expression of PIN, and upregulated expression of SERCA. These changes further support our findings in vitro and in vivo that celiprolol attenuates cardiac hypertrophy and improves heart function partially by increasing the release of NO.

### Discussion

Our study demonstrated that celiprolol attenuates cardiac myocyte hypertrophy both in vitro and in vivo and halts the

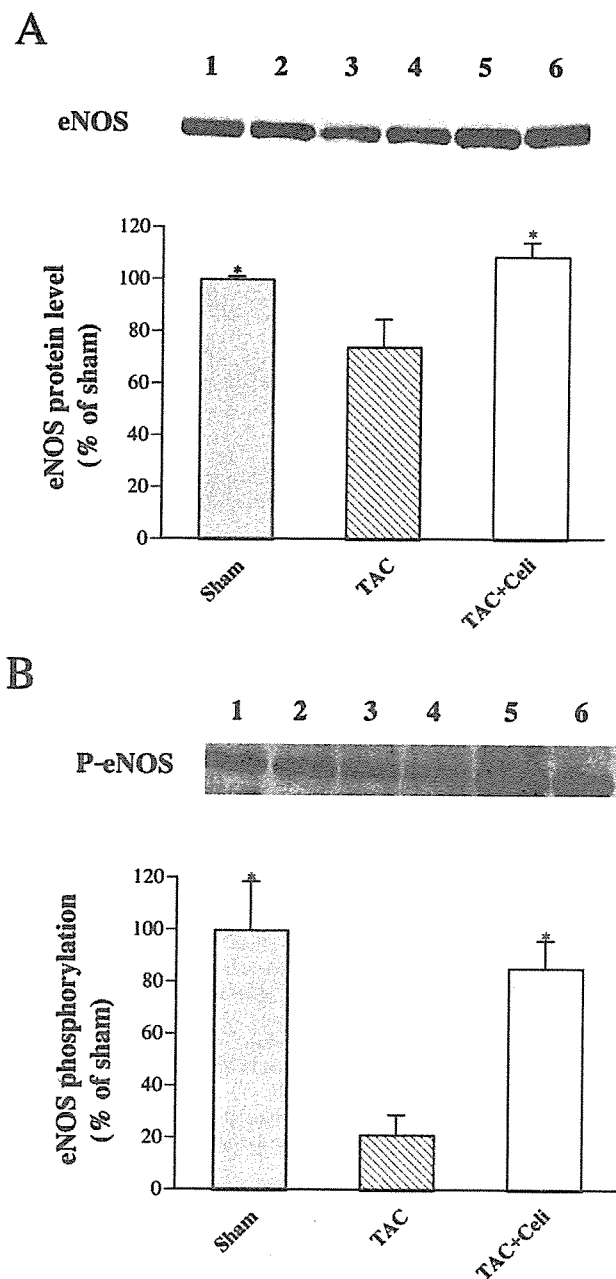


**Figure 6.** Effect of celiprolol ( $100 \text{ mg} \cdot \text{kg}^{-1} \cdot \text{d}^{-1}$ ) treatment on cardiac myocardial eNOS protein (A) and its phosphorylated activity (P-eNOS) (B). \* $P < 0.05$  vs sham.  $n = 4$  to 6 per group. Lanes 1 and 2 refer to Sham; Lanes 3 and 4, TAC; Lanes 5 and 6, TAC+Celiprolol  $100 \text{ mg} \cdot \text{kg}^{-1} \cdot \text{d}^{-1}$  in both A and B.

process leading from hypertrophy to heart failure. These effects are mediated by a selective  $\beta_1$ -AR blockade and NO-dependent pathway.

In this study, we found a negative correlation between plasma  $\text{NO}_x$  and cardiac remodeling, indicating that NO production diminished time-dependently in the process of cardiac remodeling, which is in agreement with previous reports.<sup>21–24</sup> Celiprolol inhibits cardiac remodeling via attenuating myocardial hypertrophy, decreasing cardiac fibrosis, and ameliorating pulmonary edema; this process is mediated, at least in part, by augmented eNOS signaling, because L-NAME partially abrogated this effect. Previous studies also

demonstrated that celiprolol inhibited cardiac fibrosis,<sup>25</sup> and overexpression of eNOS improved both cardiac and pulmonary function.<sup>26</sup> Although no significant difference was noted in tail-cuff pressure between the TAC mice treated with L-NAME+celiprolol and celiprolol alone, a vascular disparity really existed. Our echocardiographic data demonstrated an increase of LV chamber and myocardial hypertrophy and a decrease of LV ejection fraction in L-NAME+celiprolol-treated mice, indicating an increase of LV resistance.

The main finding in this study is that celiprolol inhibits the myocyte hypertrophy via activation of the NO signaling pathway. Experimental<sup>27</sup> and clinical<sup>28</sup> studies have also shown that activation of the NO-dependent pathway attenuates the effect of submaximal concentrations of catecholamines in the heart. These findings serve to support the results of the present study that PE-induced myocyte hypertrophy can be inhibited by celiprolol via the NO signaling pathway. Because stimulation of the adrenergic system is also involved in the pathogenesis of LV hypertrophy induced by pressure overload,<sup>29</sup> activation of the NO-dependent pathway by celiprolol should make some contribution to the attenuation of hypertrophy shown in our *in vivo* study.

Furthermore, ours is the first evidence that celiprolol can downregulate PIN, one of the potential mechanisms for the antihypertrophic effect of celiprolol. PIN has attracted significant attention for its potential importance as a regulator of nNOS,<sup>30</sup> and it also inhibits another 2 types of NOS isoenzymes (eNOS and iNOS).<sup>31</sup> The mechanisms for the linkage of  $\beta_1$ -blockade to eNOS upregulation have been clarified by other investigators. Kalinowski et al<sup>10</sup> demonstrated that some  $\beta$ -blockers augment NO production via activation of ATP efflux, with consequent stimulation of  $\text{P}_2\text{Y}$  purinoceptor. Celiprolol was also reported to activate eNOS through the PI3K-Akt signaling pathway.<sup>18</sup> Conversely, the impact on PIN may be a specific effect of  $\beta_1$ -blockers. It was reported that an association exists between nNOS decrease in the hypothalamus and enhanced sympathetic tone in rats with heart failure.<sup>32</sup> Because  $\beta_1$ -blockers are known to reduce sympathetic tone, it seems plausible that upregulation of nNOS via inhibiting PIN may make some contribution to the sympathetic inhibition of  $\beta_1$ -blockers.

We showed in this study that celiprolol completely inhibited the decrease in myocardial eNOS protein levels, whereas its inhibition was partial in plasma  $\text{NO}_x$  levels. This discrepancy might be likely. In the chronic heart failure state, in addition to the reduced myocardial eNOS expression, platelet-derived NO production<sup>33</sup> and nNOS expression in neural tissue was also reported to be decreased.<sup>34,35</sup> However, there seems to be no evidence to show that celiprolol can completely inhibit the decrease in platelet-derived NO production or nNOS expression in neural tissue, which may be one reason that celiprolol only partially prevented the plasma  $\text{NO}_x$  decrease in TAC mice.

Considering its excellent level of safety,<sup>36</sup> the favorable effect on serum lipid metabolism and insulin sensitivity in chronic heart failure,<sup>37</sup> the benefit from the blockade of  $\beta_1$ -ARs confirmed in large-scale clinical trials,<sup>38</sup> and its ability to activate the eNOS signaling pathway, a further

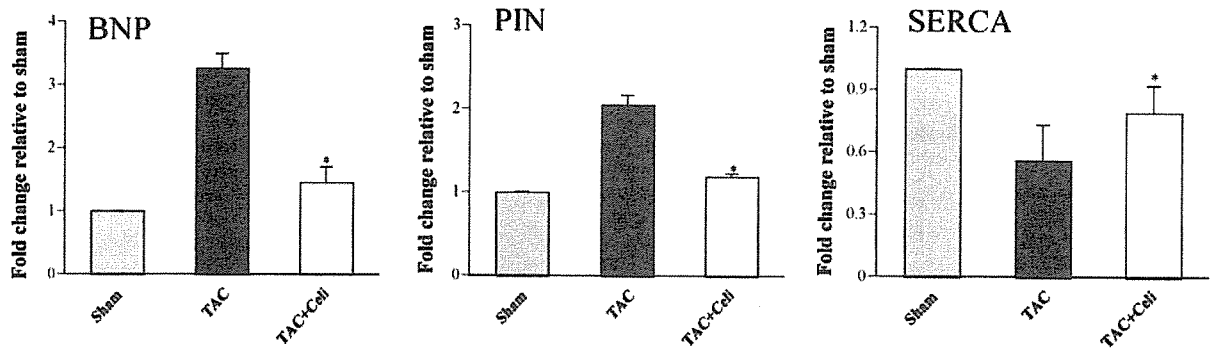


**Figure 7.** Results of real-time PCR. GAPDH was used as an endogenous control reference. Fold change was displayed as relative to sham. \* $P < 0.05$  vs TAC. Dose of celiprolol is  $100 \text{ mg} \cdot \text{kg}^{-1} \cdot \text{d}^{-1}$ ;  $n = 4$  in each group.

large-scale and long-term clinical trial is needed to provide conclusive evidence for the effect of celiprolol in patients with chronic heart failure, especially those with hypertension, cardiac hypertrophy, diabetes mellitus, or hyperlipidemia.

### Acknowledgments

This work was supported by Grants-in-Aid for Human Genome, Tissue Engineering, and Food Biotechnology (H13-Genome-011), Health and Labor Sciences Research Grants, and Comprehensive Research on Aging and Health (H13-21seiki [seikatsu]-23), Health and Labor Sciences Research Grants from Ministry of Health, Labor, and Welfare, Japan.

### References

- Friddle CJ, Koga T, Rubin EM, et al. Expression profiling reveals distinct sets of genes altered during induction and regression of cardiac hypertrophy. *Proc Natl Acad Sci U S A*. 2000;97:6745–6750.
- Morisco C, Zebrowski DC, Vatner DE, et al. Beta-adrenergic cardiac hypertrophy is mediated primarily by the beta(1)-subtype in the rat heart. *J Mol Cell Cardiol*. 2001;33:561–573.
- Gottdiener JS, Reda DJ, Massie BM, et al. Effect of single-drug therapy on reduction of left ventricular mass in mild to moderate hypertension: comparison of six antihypertensive agents. The Department of Veterans Affairs Cooperative Study Group on Antihypertensive Agents. *Circulation*. 1997;95:2007–2014.
- Calderone A, Thaik CM, Takahashi N, et al. Nitric oxide, atrial natriuretic peptide, and cyclic GMP inhibit the growth-promoting effects of norepinephrine in cardiac myocytes and fibroblasts. *J Clin Invest*. 1998;101:812–818.
- Scherrer-Crosbie M, Ullrich R, Bloch KD, et al. Endothelial nitric oxide synthase limits left ventricular remodeling after myocardial infarction in mice. *Circulation*. 2001;104:1286–1291.
- Linz W, Wohlfart P, Scholkens BA, et al. Interactions among ACE, kinins and NO. *Cardiovasc Res*. 1999;43:549–561.
- Takemoto M, Node K, Nakagami H, et al. Statins as antioxidant therapy for preventing cardiac myocyte hypertrophy. *J Clin Invest*. 2001;108:1429–1437.
- Hayashidani S, Tsutsui H, Shiomi T, et al. Fluvastatin, a 3-hydroxy-3-methylglutaryl coenzyme A reductase inhibitor, attenuates left ventricular remodeling and failure after experimental myocardial infarction. *Circulation*. 2002;105:868–873.
- Ogita H, Node K, Liao Y, et al. Raloxifene prevents cardiac hypertrophy and dysfunction in pressure-overloaded mice. *Hypertension*. 2004;43:237–242.
- Kalinowski L, Dobrucki LW, Szczepanska-Konkel M, et al. Third-generation  $\beta$ -blockers stimulate nitric oxide release from endothelial cells through ATP efflux: a novel mechanism for antihypertensive action. *Circulation*. 2003;107:2747–2752.
- Asanuma H, Node K, Minamino T, et al. Celiprolol increases coronary blood flow and reduces severity of myocardial ischemia via nitric oxide release. *J Cardiovasc Pharmacol*. 2003;41:499–505.
- Sanada S, Node K, Minamino T, et al. Long-acting  $\text{Ca}^{2+}$  blockers prevent myocardial remodeling induced by chronic NO inhibition in rats. *Hypertension*. 2003;41:963–967.
- Asakura M, Kitakaze M, Takashima S, et al. Cardiac hypertrophy is inhibited by antagonism of ADAM12 processing of HB-EGF: metalloproteinase inhibitors as a new therapy. *Nat Med*. 2002;8:35–40.
- Liao Y, Ishikura F, Beppu S, et al. Echocardiographic assessment of LV hypertrophy and function in aortic-banded mice: necropsy validation. *Am J Physiol*. 2002;282:H1703–H1708.
- Liao Y, Takashima S, Asano Y, et al. Activation of adenosine  $A_1$  receptor attenuates cardiac hypertrophy and prevents heart failure in murine left ventricular pressure-overload model. *Circ Res*. 2003;93:759–766.
- Kurusu S, Ozono R, Oshima T, et al. Cardiac angiotensin II type 2 receptor activates the kinin/NO system and inhibits fibrosis. *Hypertension*. 2003;41:99–107.
- Kitakaze M, Node K, Minamino T, et al. Role of nitric oxide in regulation of coronary blood flow during myocardial ischemia in dogs. *J Am Coll Cardiol*. 1996;27:1804–1812.
- Kobayashi N, Mita S, Yoshida K, et al. Celiprolol activates eNOS through the PI3K-Akt pathway and inhibits VCAM-1 via NF- $\kappa$ B induced by oxidative stress. *Hypertension*. 2003;42:1004–1013.
- Asano Y, Takashima S, Asakura M, et al. Lamr1 functional retroposon causes right ventricular dysplasia in mice. *Nat Genet*. 2004;36:123–130.
- Silvagno F, Xia H, Bredt DS. Neuronal nitric-oxide synthase- $\mu$ , an alternatively spliced isoform expressed in differentiated skeletal muscle. *J Biol Chem*. 1996;271:11204–11208.
- Yu CM, Fung PC, Chan G, et al. Plasma nitric oxide level in heart failure secondary to left ventricular diastolic dysfunction. *Am J Cardiol*. 2001;88:867–870.
- Tonduangu D, Hittinger L, Ghaleh B, et al. Chronic infusion of bradykinin delays the progression of heart failure and preserves vascular endothelium-mediated vasodilation in conscious dogs. *Circulation*. 2004;109:114–119.
- Katz SD, Khan T, Zeballos GA, et al. Decreased activity of the L-arginine-nitric oxide metabolic pathway in patients with congestive heart failure. *Circulation*. 1999;99:2113–2117.
- Agnoletti L, Currello S, Bachetti T, et al. Serum from patients with severe heart failure downregulates eNOS and is proapoptotic: role of tumor necrosis factor- $\alpha$ . *Circulation*. 1999;100:1983–1991.
- Kobayashi N, Mori Y, Nakano S, et al. Celiprolol stimulates endothelial nitric oxide synthase expression and improves myocardial remodeling in deoxycorticosterone acetate-salt hypertensive rats. *J Hypertens*. 2001;19:795–801.
- Jones SP, Greer JJ, van Haperen R, et al. Endothelial nitric oxide synthase overexpression attenuates congestive heart failure in mice. *Proc Natl Acad Sci U S A*. 2003;100:4891–4896.
- Balligand JL, Kelly RA, Marsden PA, et al. Control of cardiac muscle cell function by an endogenous nitric oxide signaling system. *Proc Natl Acad Sci U S A*. 1993;90:347–351.
- Hare JM, Keaney JF Jr, Balligand JL, et al. Role of nitric oxide in parasympathetic modulation of beta-adrenergic myocardial contractility in normal dogs. *J Clin Invest*. 1995;95:360–366.
- Reaven GM, Lithell H, Landsberg L. Hypertension and associated metabolic abnormalities: the role of insulin resistance and the sympathoadrenal system. *N Engl J Med*. 1996;334:374–381.

30. Jaffrey SR, Snyder SH. PIN: an associated protein inhibitor of neuronal nitric oxide synthase. *Science*. 1996;274:774-777.
31. Hemmens B, Woschitz S, Pitters E, et al. The protein inhibitor of neuronal nitric oxide synthase (PIN): characterization of its action on pure nitric oxide synthases. *FEBS Lett*. 1998;430:397-400.
32. Patel KP, Zhang K, Zucker IH, et al. Decreased gene expression of neuronal nitric oxide synthase in hypothalamus and brainstem of rats in heart failure. *Brain Res*. 1996;734:109-115.
33. Dixon LJ, Morgan DR, Hughes SM, et al. Functional consequences of endothelial nitric oxide synthase uncoupling in congestive cardiac failure. *Circulation*. 2003;107:1725-1728.
34. Zhang K, Li YF, Patel KP. Blunted nitric oxide-mediated inhibition of renal nerve discharge within PVN of rats with heart failure. *Am J Physiol*. 2001;281:H995-H1004.
35. Hirooka Y, Shigematsu H, Kishi T, et al. Reduced nitric oxide synthase in the brainstem contributes to enhanced sympathetic drive in rats with heart failure. *J Cardiovasc Pharmacol*. 2003;42(suppl 1):S111-S115.
36. Witchitz S, Cohen-Solal A, Dartois N, et al. Treatment of heart failure with celiprolol, a cardioselective beta blocker with beta-2 agonist vasodilatory properties. The CELICARD Group. *Am J Cardiol*. 2000;85:1467-1471.
37. Pietila M, Malminiemi K, Huupponen R, et al. Celiprolol augments the effect of physical exercise on insulin sensitivity and serum lipid levels in chronic heart failure. *Eur J Heart Fail*. 2000;2:81-90.
38. Waagstein F, Bristow MR, Swedberg K, et al. Beneficial effects of metoprolol in idiopathic dilated cardiomyopathy. Metoprolol in Dilated Cardiomyopathy (MDC) Trial Study Group. *Lancet*. 1993;342:1441-1446.

# Protein Kinase A as Another Mediator of Ischemic Preconditioning Independent of Protein Kinase C

Shoji Sanada, MD, PhD; Hiroshi Asanuma, MD, PhD; Osamu Tsukamoto, MD; Tetsuo Minamino, MD, PhD; Koichi Node, MD, PhD; Seiji Takashima, MD, PhD; Tomi Fukushima, PhD; Akiko Ogai, PhD; Yoshiro Shinozaki, MD, PhD; Masashi Fujita, MD; Akio Hirata, MD; Hiroko Okuda, MD; Hiroaki Shimokawa, MD, PhD; Hitonobu Tomoike, MD, PhD; Masatsugu Hori, MD, PhD; Masafumi Kitakaze, MD, PhD

**Background**—We and others have reported that transient accumulation of cyclic AMP (cAMP) in the myocardium during ischemic preconditioning (IP) limits infarct size independent of protein kinase C (PKC). Accumulation of cAMP activates protein kinase A (PKA), which has been demonstrated to cause reversible inhibition of RhoA and Rho-kinase. We investigated the involvement of PKA and Rho-kinase in the infarct limitation by IP.

**Methods and Results**—Dogs were subjected to 90-minute ischemia and 6-hour reperfusion. We examined the effect on Rho-kinase activity during sustained ischemia and infarct size of (1) preischemic transient coronary occlusion (IP), (2) preischemic activation of PKA/PKC, (3) inhibition of PKA/PKC during IP, and (4) inhibition of Rho-kinase or actin cytoskeletal deactivation during myocardial ischemia. Either IP or dibutyl-*c*-AMP treatment activated PKA, which was dose-dependently inhibited by 2 PKA inhibitors (H89 and Rp-cAMP). IP and preischemic PKA activation substantially reduced infarct size, which was blunted by preischemic PKA inhibition. IP and preischemic PKA activation, but not PKC activation, caused a substantial decrease of Rho-kinase activation during sustained ischemia. These changes were cancelled by preischemic inhibition of PKA but not PKC. Furthermore, either Rho-kinase inhibition (hydroxyfasudil or Y27632) or actin cytoskeletal deactivation (cytochalasin-D) during sustained ischemia achieved the same infarct limitation as preischemic PKA activation without affecting systemic hemodynamic parameters, the area at risk, or collateral blood flow.

**Conclusions**—Transient preischemic activation of PKA reduces infarct size through Rho-kinase inhibition and actin cytoskeletal deactivation during sustained ischemia, implicating a novel mechanism for cardioprotection by ischemic preconditioning independent of PKC and a potential new therapeutic target. (*Circulation*. 2004;110:51-57.)

**Key Words:** ischemia ■ infarction ■ proteins

The potent cardioprotection induced by brief periods of ischemia before sustained ischemia is termed ischemic preconditioning (IP). Previous studies<sup>1-4</sup> have exhibited some possible mediators of IP-derived cardioprotection, suggested to link with protein kinase C (PKC).<sup>3,4</sup> On the other hand, a brief preconditioning ischemia also induces a synchronized increase of the myocardial cyclic AMP (cAMP) level.<sup>5</sup> Furthermore, we and others<sup>5,6</sup> have reported that brief preischemic exposure to  $\beta$ -agonists, an adenylate cyclase activator, phosphodiesterase type III inhibitors, or a cell-permeable cAMP analogue, all of which cause rapid activation of protein kinase A (PKA), also protects the myocardium in vivo independently of

PKC. However, little is known about the direct contribution of PKA to infarct limitation by IP and the associated subcellular mechanisms. Some recent studies have demonstrated that an increase of cAMP followed by activation of PKA causes temporary inhibition of small GTPase RhoA<sup>7,8</sup> and its downstream Rho-kinase,<sup>7</sup> playing major roles in enhancement of actin cytoskeleton formation followed by chemotactic migration, platelet activation, and cytokinesis.<sup>7,9</sup> Therefore, we hypothesized that transient preischemic activation of PKA may also cause IP-induced infarct limitation through the inhibition of Rho-kinase after the onset of sustained ischemia. This study was designed to test this hypothesis in vivo.

Received November 15, 2003; de novo received December 28, 2003; revision received March 10, 2004; accepted March 17, 2004.

From the Department of Internal Medicine and Therapeutics, Osaka University Graduate School of Medicine, Suita; Cardiovascular Division (K.N.), Department of Medicine, Saga University Faculty of Medicine, Saga; Cardiovascular Division of Medicine (A.O., H.T., M.K.), National Cardiovascular Center, Suita; Department of Physiological Science (Y.S.), Tokai University School of Medicine, Isehara; and Department of Cardiovascular Medicine (H.S.), Kyushu University Graduate School of Medical Sciences, Fukuoka, Japan.

Presented in part at the 76th Scientific Sessions of the American Heart Association, Orlando, FL, November 9-12, 2003, and published as an abstract (*Circulation*. 2003;108(suppl IV):IV-186).

Correspondence to Masafumi Kitakaze, MD, PhD, Cardiovascular Division of Medicine, National Cardiovascular Center, 5-7-1 Fujishirodai, Suita, 565-8565 Japan. E-mail kitakaze@zf6.so-net.ne.jp

© 2004 American Heart Association, Inc.

*Circulation* is available at <http://www.circulationaha.org>

DOI: 10.1161/01.CIR.0000133390.12306.C7

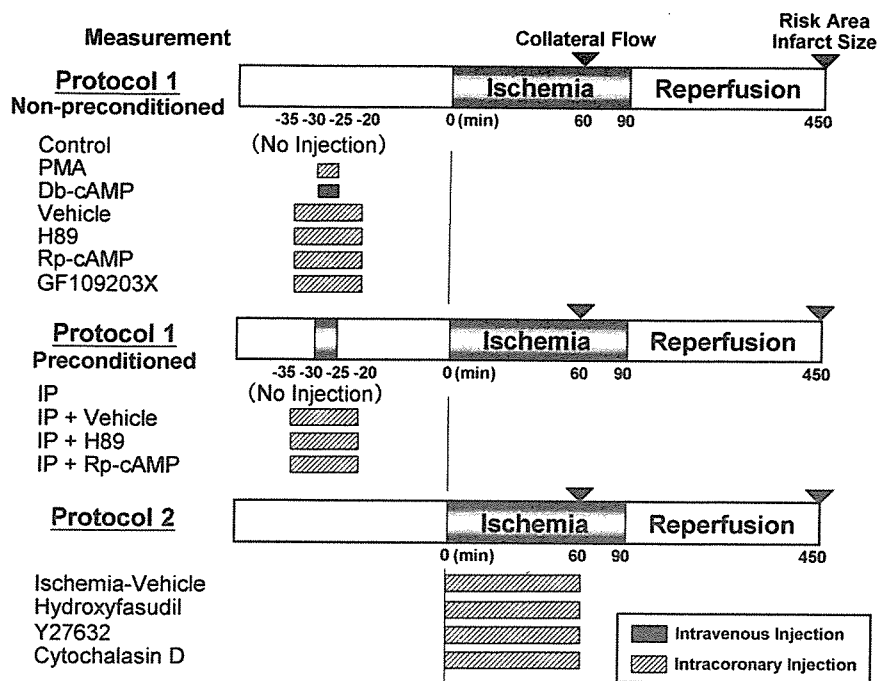


Figure 1. Protocols for measuring infarct size.

## Methods

All procedures were performed in conformity with the *Guide for the Care and Use of Laboratory Animals* (NIH Publication No. 85-23, 1996 revision) and were approved by the Osaka University Committee for Laboratory Animal Use.

### Instrumentation

As described previously,<sup>10</sup> beagle dogs (Oriental Yeast; Osaka, Japan) weighing 9 to 14 kg were anesthetized with sodium pentobarbital (30 mg/kg IV) and connected to an extracorporeal bypass tube. In all experiments, the average control values of mean aortic blood pressure (ABP), heart rate (HR), and arterial blood  $pO_2$  were  $101 \pm 2.3$  mm Hg,  $127 \pm 2.4$ /minute, and  $108 \pm 3.8$  mm Hg, respectively. Both ABP and HR were measured continuously during the experiment.

### Experimental Protocols

#### Protocol 1: Infarct Size After Preconditioning

Figure 1 shows the study protocol. After hemodynamic stabilization, 176 dogs underwent 90 minutes of ischemia and 6 hours of reperfusion with or without 1 or more of the following interventions: (1) 5-minute coronary occlusion followed by 25-minute reperfusion just before sustained ischemia (IP), (2) intracoronary administration of the potent PKC activator phorbol 12-myristate 13-acetate (PMA, Sigma; 0.62 ng/kg per min), or (3) an intravenous administration of the cell-permeable cAMP analogue dibutyryl-cAMP (db-cAMP, Sigma; 5 mg/kg over 5 minutes), in combination with (4) intracoronary injection of a selective PKC inhibitor, GF109203X (Calbiochem; 40  $\mu$ g/kg per min) or 1 of 2 selective PKA inhibitors (H89<sup>6,11</sup> [Sigma; 1.35  $\mu$ g/kg per min] or the Rp-isomer of cAMP<sup>12</sup> [Rp-cAMP, Calbiochem; 45  $\mu$ g/kg per min]) or (5) infusion of vehicle (at a rate of 0.0167 mL/kg per min) (control, vehicle, IP, IP+vehicle, IP+H89, IP+Rp-cAMP, PMA, PMA+H89, PMA+Rp-cAMP, Db-cAMP, Db-cAMP+H89, Db-cAMP+Rp-cAMP, Db-cAMP+GF109203X [GFX], PMA+Db-cAMP, H89, Rp-cAMP, and GFX groups, respectively; n=8 to 13 each).

We used the same PMA or db-cAMP regimens that were used in our previous studies,<sup>3,6</sup> which demonstrated potent infarct limitation in this model. The regimen of GF109203X infusion was the same as that used in our previous study<sup>3</sup> to blunt infarct limitation by IP and PMA.

#### Protocol 2: Infarct Size in the Inhibition Protocol During Ischemia

The lower part of Figure 1 shows the protocol. Sixty-six dogs underwent the same protocol for sustained ischemia-reperfusion with or without intracoronary administration of (1) a selective Rho-kinase inhibitor (hydroxyfasudil<sup>13</sup> [Asahi-Kasei; 2.4 and 12  $\mu$ g/kg per min] or Y27632<sup>14</sup> [Welfide; 0.7 and 3.5  $\mu$ g/kg per min]), (2) an actin cytoskeleton disruptor cytochalasin-D<sup>15</sup> (Calbiochem; 5.1  $\mu$ g/kg per min), or (3) vehicle (a small volume of DMSO, which does not affect infarct size in the same model<sup>10</sup>) between the onset and 60 minutes of sustained ischemia (hydroxyfasudil-lower dose [LD], hydroxyfasudil, Y27632-LD, Y27632, cytochalasin-D, and ischemia-vehicle groups, respectively; n=10 to 12 each).

The higher doses of hydroxyfasudil and Y-27632 for intracoronary infusion were the highest doses that could not influence systemic hemodynamics during our preliminary study in this model (data not shown).

#### Protocol 3: Tissue Kinase Assay

Figure 2 shows the protocol. Ninety dogs were subjected to sustained myocardial ischemia according the same method as in protocol 1 with or without (1) IP, (2) preischemic administration of db-cAMP or PMA, (3) preischemic administration of H89, Rp-cAMP, or GF109203X, or (4) administration of hydroxyfasudil or Y27632 during ischemia (sham, control, PMA, Db-cAMP, ischemia-vehicle, hydroxyfasudil-LD, hydroxyfasudil, Y27632-LD, Y27632, Db-cAMP+Rp-cAMP, IP, IP+vehicle, IP+H89, IP+Rp-cAMP, and IP+GF109203X groups, respectively; n=4 or 5 each).

We quickly sampled the myocardium in the target region (1) at the end of IP, PMA infusion, or db-cAMP infusion to assay PKA and (2) after 60-minute ischemia to assay Rho-kinase activity (Figure 2). The sampled tissues were rapidly frozen in liquid nitrogen and stored at  $-80^\circ\text{C}$ .

### Measurements of Collateral Blood Flow, Risk Area, and Infarct Size

In protocols 1 and 2, we measured the myocardial collateral blood flow after 60 minutes of ischemia by a nonradioactive microsphere method and evaluated both the area at risk and the infarct size by dual staining, as described previously.<sup>6,10</sup>



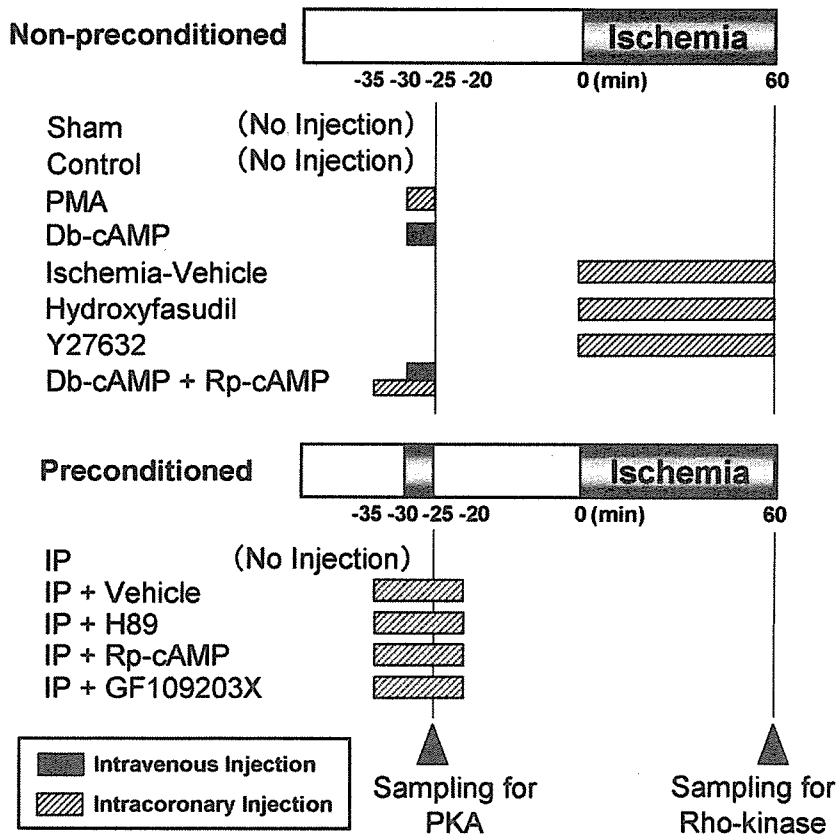


**Figure 2.** Protocols for measuring PKA/Rho-kinase activities. Samples for PKA and Rho-kinase in each group are prepared separately.

### Exclusion Criteria

To ensure that all of the animals included in the data analysis were healthy and were exposed to a similar extent of ischemia, the exclusion criteria described previously<sup>10</sup> regarding hemodynamics, excessive collateral flow, and lethal arrhythmia were used.

### PKA and Rho-Kinase Assay

We assayed PKA and Rho-kinase activity as described previously<sup>13,16</sup> with some modifications, using specific antibodies for a substrate of PKA (phospho-CREB [Upstate Biology]) or Rho-kinase (myosin phosphatase targeting subunit [MYPT]-1 [Upstate Biotechnology]) and phospho-MYPT-1 [Thr696; Upstate Biotechnology]) as the primary antibodies. Rho-kinase activity was determined as the phosphorylated ratio of MYPT.

### Statistical Analysis

Results are expressed as mean $\pm$ SEM. Statistical analysis was performed by ANOVA with modified Bonferroni's post hoc test, and significance was defined at  $P < 0.05$ .

## Results

### Mortality and Exclusions, Hemodynamic

#### Parameters, Risk Area, and Collateral Blood Flow

Among the 242 dogs used in protocols 1 and 2, 55 dogs met the exclusion criteria of ventricular fibrillation or excessive myocardial collateral blood flow ( $>15$  mL/100 g per min). Therefore, 187 dogs completed these protocols satisfactorily and were included in the data analysis (Table). The changes of ABP and HR were comparable among the 23 groups throughout the experiment (data not shown), and the area at risk and collateral blood flow were also comparable (Table).

### Infarct Size

Figure 3 shows the infarct size for each group in protocol 1 (left) and protocol 2 (right). In protocol 1, IP ( $11.9 \pm 2.1\%$  in the IP group and  $14.8 \pm 2.1\%$  in the IP+vehicle group) as well as preischemic treatment with PMA and Db-cAMP in combination ( $14.0 \pm 2.6\%$  in the PMA+Db-cAMP group) markedly exhibited infarct limitation, which were more potent than either PMA ( $17.3 \pm 2.5\%$ ) or db-cAMP ( $20.1 \pm 2.2\%$ ) alone but did not reach a significant difference. Infarct size in these 4 groups was significantly smaller ( $P < 0.05$  each) than that in either the control ( $40.1 \pm 3.8\%$ ) or vehicle ( $40.6 \pm 3.6\%$ ) group. Treatment with either H89 or Rp-cAMP during preconditioning similarly blunted the infarct limitation by IP ( $33.4 \pm 3.8\%$  and  $34.1 \pm 4.1\%$ , respectively; both  $P < 0.05$  versus IP and not significant versus control) and db-cAMP ( $37.4 \pm 3.6\%$  and  $39.1 \pm 3.9\%$ , respectively; both  $P < 0.05$  versus the db-cAMP group), whereas these agents did not affect PMA-induced infarct limitation ( $19.2 \pm 3.0\%$  and  $18.5 \pm 2.7\%$ , respectively; both  $P < 0.05$  versus control). Furthermore, infarct limitation by db-cAMP was not affected by the effective dose of GF109203X ( $20.8 \pm 3.1\%$ ,  $P < 0.05$  each versus control) in this model.<sup>5</sup> H89, Rp-cAMP, and GF109203X alone did not affect infarct size ( $42.7 \pm 4.2\%$ ,  $38.6 \pm 4.6\%$ , and  $41.9 \pm 4.5\%$ , respectively) (Figure 3). In protocol 2 (Figure 3, right), administration of the vehicle during ischemia did not influence infarct size ( $43.4 \pm 4.4\%$ ), the area at risk, or collateral blood flow (Table 1) compared with the control group. Administration of either hydroxyfasudil or Y27632 during sustained ischemia caused dose-dependent infarct limitation like that attributable to preische-

Profile of the Groups in Protocols 1 and 2

Groups	Excluded							
	Initial No.	Lethal Arrhythmia			Excessive Collateral Flow	Final No.	Area at Risk, %	Collateral Flow, mL/100 g per min
		During Ischemia	After Reperfusion					
Control	13	0	2	1	10	39.8±2.2	8.3±0.9	
Vehicle	12	1	1	0	10	40.5±1.6	9.1±1.2	
IP	9	0	0	1	8	39.6±2.2	9.4±1.3	
IP+ vehicle	10	0	0	2	8	40.8±2.2	9.0±1.2	
PMA	11	1	0	2	8	39.0±1.9	9.1±1.3	
Db-cAMP	13	0	1	2	10	38.6±1.9	9.3±1.4	
PMA+Db-cAMP	10	0	0	2	8	40.1±2.1	9.1±1.5	
IP+H89	10	0	2	0	8	40.3±1.7	8.5±0.9	
IP+Rp-cAMP	11	0	2	1	8	39.2±1.7	9.1±1.2	
PMA+H89	11	0	2	1	8	39.4±1.8	8.7±1.4	
PMA+Rp-cAMP	10	1	0	1	8	39.7±2.1	9.1±1.4	
Db-cAMP+H89	9	0	1	0	8	41.0±2.1	8.6±1.3	
Db-cAMP+Rp-cAMP	10	0	1	1	8	39.9±1.5	8.4±1.4	
Db-cAMP+GFX	10	0	0	2	8	38.7±1.6	9.0±1.5	
H89	9	0	2	0	7	41.1±1.8	8.6±1.1	
Rp-cAMP	10	0	2	1	7	39.8±1.9	9.0±1.4	
GFX	8	0	1	0	7	40.8±2.2	8.2±1.3	
Ischemia-vehicle	11	1	2	0	8	41.4±2.1	8.6±1.1	
Hydroxyfasudil-LD	10	1	0	1	8	38.4±2.6	8.9±1.6	
Hydroxyfasudil	11	0	0	3	8	38.1±2.5	9.5±1.5	
Y27632-LD	10	0	0	2	8	38.5±2.5	9.2±1.2	
Y27632	12	0	0	4	8	37.8±2.8	9.8±1.7	
Cytochalasin-D	12	0	1	3	8	38.0±2.4	9.4±1.6	

Mortality, exclusion, area at risk, and collateral flow in each group in protocols 1 and 2. Data are expressed as mean±SEM.

mic PKA activation (30.5±5.3% and 22.0±4.1% in the hydroxyfasudil-LD and hydroxyfasudil groups, respectively; 30.0±5.3% and 21.7±3.9% in the Y27632-LD and Y27632 groups, respectively). Only the higher dose of each agent achieved significant (both  $P<0.05$ ) infarct limitation, showing that these were the minimum doses to exert a sufficient effect in this model. Cytochalasin-D also similarly reduced the infarct size (22.9±4.4%,  $P<0.05$  versus control).

### PKA Activity During Preconditioning

In protocol 3, IP and db-cAMP activated PKA (267±22% and 288±34% of baseline, respectively; both  $P<0.05$  versus sham). IP-derived PKA activation was inhibited by coadministration of H89 or Rp-cAMP (112±23% and 99±17%, respectively; both  $P<0.05$  versus IP+vehicle). We also confirmed that Db-cAMP-derived PKA activation was cancelled by Rp-cAMP (121±22%,  $P<0.05$  versus IP+vehicle). Furthermore, we observed that 1 to 5 doses of H89 and Rp-cAMP only caused partial (189±29% and 175±29%, respectively) inhibition of PKA (Figure 4), showing that the dose levels we used in this study were the minimum effective doses, which should eliminate the possibility of a nonspecific action in this model.

### Rho-Kinase Activity During Ischemia

A 60-minute period of ischemia caused Rho-kinase activation (307±25% of baseline in the control group;  $P<0.05$  versus

sham), which was attenuated by IP or preischemic administration of db-cAMP (145±21% and 151±26%, respectively;  $P<0.05$  versus control) but not by PMA (253±30%,  $P<0.05$  versus sham). The IP-induced suppression of Rho-kinase activation was cancelled by Rp-cAMP (247±39%,  $P<0.05$  versus IP) but not by GF109203X (161±34%,  $P<0.05$  versus control) at the same dose as in protocol 1 (Figure 5; left). Furthermore, administration of either hydroxyfasudil or Y27632 during sustained ischemia caused a dose-dependent decrease of Rho-kinase activation (199±36% and 205±33% in the hydroxyfasudil-LD and Y27632-LD groups, respectively; 134±21% and 135±20% in the hydroxyfasudil and Y27632 groups, respectively), which was significant ( $P<0.05$  versus the ischemia-vehicle group) at the higher doses (Figure 5; right).

## Discussion

### Triggers of IP: Involvements of cAMP, PKA, and $\beta$ -Adrenoceptors

Single or repeated IP as well as repeated treatment with forskolin is reported to rapidly and transiently increase both myocardial cAMP level and tissue PKA activity.<sup>5</sup> We observed in this model that the intracoronary coadministration of different types of selective PKA antagonists blunted infarct

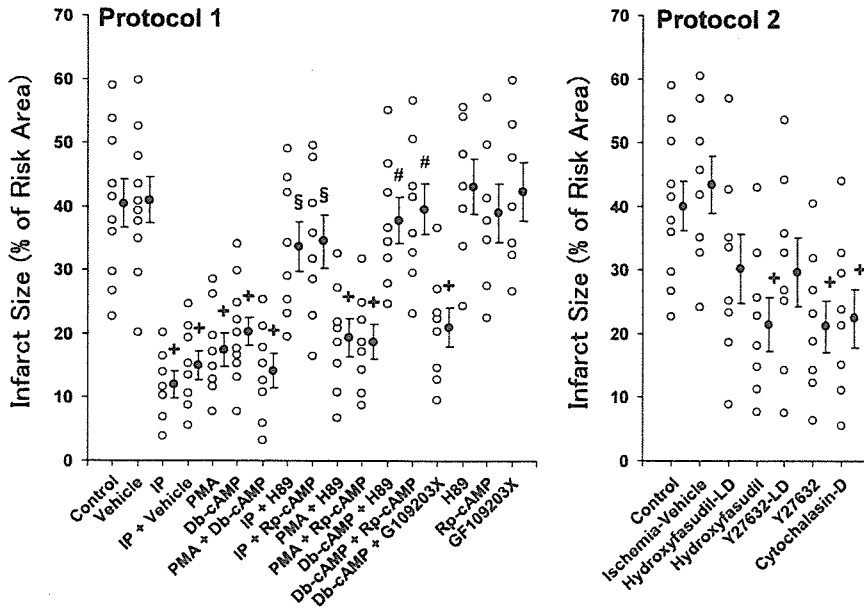


**Figure 3.** Infarct size in the groups in protocols 1 and 2. +*P*<0.05 vs control. §*P*<0.05 vs IP.

limitation of IP, suggesting the involvement of PKA in the IP-derived cardioprotection. However, it remains unclear whether the  $\beta$ -adrenoceptor is involved in this response, despite the prominent role of the  $\alpha_1$ -adrenoceptor in PKC-mediated cardioprotection.<sup>1,5</sup> Although a single exposure to brief ischemia or a  $\beta$ -agonist limits infarct size through  $\beta$ -adrenoceptor activation<sup>5,17</sup> and repeated preischemic activation of the cAMP-PKA-dependent pathway is also modulated by  $\beta$ -adrenoceptor expression,<sup>18</sup> the contribution of this receptor in cardioprotection by repeated exposures remains unclear<sup>5,17</sup> because of PKA-induced rapid desensitization.<sup>19</sup> It is reported in other systems that the repeated IP might lead to cAMP accumulation and direct PKA activation independently of the  $\beta$ -adrenoceptor<sup>5</sup> through the inhibition of phosphodiesterase<sup>5</sup> or direct sensitization of adenylate cyclase.<sup>20</sup> However, we have documented preliminarily in the present model that the intracoronary coadministration of the

selective ultra-short-acting  $\beta_1$ -adrenoceptor blocker landiolol<sup>21</sup> around the preconditioning ischemia (as in protocol 1) blunted the infarct limitation by IP used in this study ( $35.0 \pm 4.4\%$ ,  $n=7$ ) as well as PKA inhibitors during IP, additionally suggesting the essential contribution of  $\beta_1$ -adrenoceptor activation to cause IP-induced PKA-dependent cardioprotection in this model. However, more studies might be expected to clarify these issues.

On the other hand, IP leads to decreased cAMP accumulation during sustained ischemia,<sup>22</sup> but it is controversial whether this explains the cardioprotection afforded by preischemic activation of PKA.<sup>5,22</sup> Enhancement of cAMP accumulation during sustained ischemia fails to block cardioprotection by IP.<sup>22</sup> Moreover, overexpression of  $\beta$ -adrenergic receptor kinase-1, which causes functional uncoupling of  $\beta$ -adrenoceptors, impairs ischemia-reperfusion injury, and this impairment is reversed by co-overexpression of  $\beta$ -adrenergic receptor kinase-1 inhibitor.<sup>23</sup>

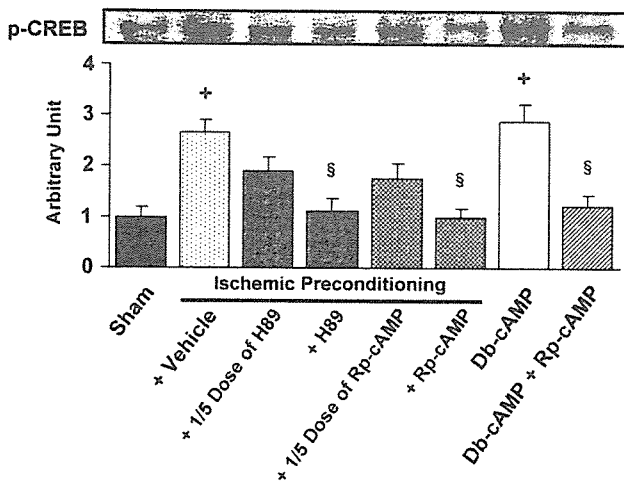


**Figure 4.** PKA activity estimated by Western blotting for phosphorylated CREB in protocol 2 (see text for details). Top, Representative specimens; bottom, average values ( $n=4$  to 5 each). +*P*<0.05 vs sham. §*P*<0.05 vs IP+vehicle.

**Role of PKA and PKC**

Manganello et al<sup>8</sup> demonstrated that PKA primarily phosphorylates the switch-I region of  $G-\alpha_{13}$  (an essential G-protein for signaling to RhoA stimulated by G-protein-coupled receptors<sup>8</sup>) and inhibits its binding with  $G-\beta-\gamma$ , which subsequently leads to the inhibition of  $G-\alpha_{13}$  turnover and inactivation of RhoA.

Although PKC<sup>24</sup> or its downstream kinase<sup>25</sup> has been reported to induce actin assembly through activation of PKC-potentiated phosphatase inhibitor and Rho-kinase, another study found that both PKC and the downstream Src tyrosine kinase rapidly deactivate RhoA through p190 and cause actin disassembly.<sup>26</sup> The PKC-Src/Lck pathway was reported to play a role in cardioprotection by IP.<sup>4</sup> However, preischemic PKC activation had little influence on IP-induced Rho-kinase inhibition in this study, showing the limited contribution of PKC to this pathway. Furthermore, we have reported<sup>27</sup> that Src/Lck tyrosine kinase is not involved in the infarct limitation by IP in this model. Although it did not

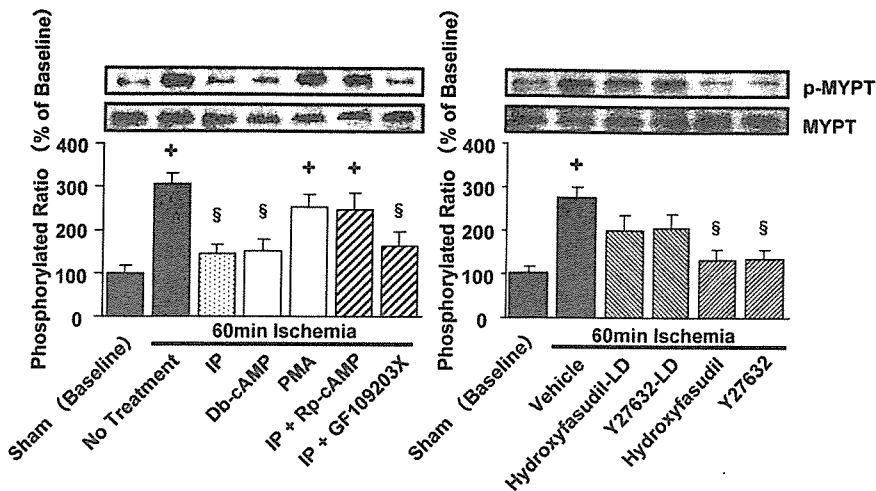


**Figure 5.** Rho-kinase activity estimated by Western blotting for MYPT-1 and phosphorylated MYPT-1 in protocol 2 (see text for details). Top, Representative specimens; bottom, average values ( $n=4$  to 5 each).  $+P<0.05$  vs sham;  $§P<0.05$  vs control.

reach statistical significance, our present data additionally imply that (1) there are multiple pathways in parallel to confer cardioprotection of IP, PKC-induced Rho-kinase-independent and PKA-induced Rho-kinase-dependent ones, or (2) PKC-induced pathway exerts stronger effects than the PKA-induced one to cause cardioprotection of IP. Given that repeated IP only promotes transient, not sustained, activation of PKC,<sup>28</sup> it is highly possible that transient activation of both PKA and PKC is independently but synergistically responsible for mediating a variety of cardioprotective pathways triggered by IP.

### Cardioprotection by Rho-Kinase Inhibition

Because inhibition of Rho-kinase directly relaxes vascular smooth muscle,<sup>9,13,29</sup> it may increase regional myocardial blood flow at sites of major coronary artery stenosis (without any inotropic or chronotropic effect) by dilating the abnormal artery.<sup>29</sup> However, this study showed that Rho-kinase inhibition during sustained ischemia exerted cardioprotection without altering hemodynamics, even after all of the dogs with excessive collateral flow were excluded from analysis. Therefore, the infarct-limiting mechanism that involves Rho-kinase inhibition could be independent of either a change in systemic hemodynamics or the recruitment of collateral blood flow.

Rho-kinase has multiple effects on the cardiovascular system, which dominantly represent those of RhoA,<sup>9</sup> because of inhibition of myosin phosphatase and activation of the ERM family (ezrin, radixin, or moesin) or adducin.<sup>9</sup> Importantly, Rho-kinase plays a major role in stress fiber formation, focal adhesion, migration, and cytokinesis through activation of the ERM family and thus can enhance cardiac damage in acute ischemia. The potent infarct limitation by cytochalasin-D that mimicked PKA-Rho-kinase-mediated cardioprotection suggests that deactivation of stress fiber polymerization is a major part of this cardioprotective mechanism.

In fact, the effect of changes to the actin cytoskeleton on infarct size has been controversial, because a previous study revealed that targeted deletion of the internal actin disruptor caused the exacerbation of ischemic damage and was rescued by cytochalasin-D,<sup>30</sup> whereas another study revealed that cytochalasin-D abolished the infarct limitation by IP.<sup>31</sup> How-

ever, inhibition of Rho and Rho-kinase has also been reported to activate endothelial NO synthase,<sup>15</sup>  $K_{ATP}$  channels,<sup>32</sup> and 5'-nucleotidase,<sup>33</sup> all of which have been reported to protect the myocardium against ischemia-reperfusion injury. Additional studies are needed to clarify such issues, because these controversies are likely to be attributable to the differences in experimental design and in the critical time window for the contribution of each factor.

Inhibition of Rho-kinase has also been shown to attenuate the production of superoxide, reduce the generation of monocyte chemoattractant protein-1 or plasminogen activator inhibitor-1, and inhibit the activation of macrophages, neutrophils, and platelets, all of which finally lead to the inhibition of stress-induced regional inflammatory responses and diminished myocardial ischemia-reperfusion injury.<sup>9</sup> IP has been reported to modulate most of these factors,<sup>1,2</sup> additionally supporting our present results. Accordingly, our preliminary data in the same model indicate that the intracoronary infusion of Y27632 (3  $\mu\text{g}/\text{kg}$  per min) for 30 minutes just after reperfusion also reduced infarct size ( $22.3 \pm 4.8\%$ ,  $n=7$ ) as expected. However, the underlying mechanism and its association with the IP-induced preischemic PKA activation should be further elucidated.

In conclusion, although additional studies will be needed before these can be used for the development of novel, safe, and effective therapies, inhibition of Rho-kinase during ischemia, long-term inhibition of Rho-kinase pharmacologically or genetically, or repeated short-term activation of  $\beta$ -adrenoceptors or PKA may also be useful.

### Acknowledgments

This study was supported by Grants on Human Genome, Tissue Engineering and Food Biotechnology (H13-Genome-11), Grants on Comprehensive Research on Aging and Health (H13-21seiki[seikatsu]-23), Health and Labor Sciences Research from the Ministry of Health, Labor and Welfare, and a Grant-in-Aid for Scientific Research from the Ministry of Education, Culture, Sports, Science and Technology of Japan and in part by Mitsubishi Pharma Research Foundation, the Japan Heart Foundation, and a Grant-in-Aid for JSPS fellows from the Japan Society for the Promotion of Science.

### References

- Sanada S, Kitakaze M. Ischemic preconditioning: emerging evidence, controversy and translational trials. *Int J Cardiol*. In press.

2. Sanada S, Kitakaze M, Asanuma H, et al. Role of the mitochondrial and sarcolemmal KATP channels in ischemic preconditioning on the canine heart. *Am J Physiol Heart Circ Physiol*. 2001;280:H256–H263.
3. Node K, Kitakaze M, Minamino T, et al. Activation of ecto-5'-nucleotidase by protein kinase-C and its role in ischaemic tolerance in the canine heart. *Br J Pharmacol*. 1997;120:273–281.
4. Ping P, Zhang J, Zheng YT, et al. Demonstration of selective protein kinase C-dependent activation of Src and Lck tyrosine kinases during ischemic preconditioning in conscious rabbits. *Circ Res*. 1999;85:542–550.
5. Lochner A, Genade S, Tromp E, et al. Ischemic preconditioning and the beta-adrenergic signal transduction pathway. *Circulation*. 1999;100:958–966.
6. Sanada S, Kitakaze M, Papst PJ, et al. Cardioprotective effect afforded by transient exposure to phosphodiesterase-III inhibitors: the role of protein kinase-A and P38 mitogen-activated protein kinase. *Circulation*. 2001;104:705–710.
7. Dong JM, Leung T, Manser E, et al. cAMP-induced morphological changes are counteracted by the activated RhoA small GTPase and the Rho kinase ROKalpha. *J Biol Chem*. 1998;273:22554–22562.
8. Manganello JM, Huang JS, Kozasa T, et al. Protein kinase A-mediated phosphorylation of the Galpha13 switch-I region alters the Galphabeta13-G protein-coupled receptor complex and inhibits Rho activation. *J Biol Chem*. 2003;278:124–130.
9. Shimokawa H. Rho-kinase as a novel therapeutic target in treatment of cardiovascular diseases. *J Cardiovasc Pharmacol*. 2002;39:319–327.
10. Sanada S, Kitakaze M, Papst PJ, et al. Role of phasic dynamism of P38 mitogen-activated protein kinase activation in the ischemic preconditioning on the canine heart. *Circ Res*. 2001;88:175–180.
11. Chijiwa T, Mishima A, Hagiwara M, et al. Inhibition of forskolin-induced neurite outgrowth and protein phosphorylation by a newly synthesized selective inhibitor of cyclic AMP-dependent protein kinase, N-[2-(p-bromocinnamylamino)ethyl]-5-isoquinoline-sulfonamide (H-89), of PC12D pheochromocytoma cells. *J Biol Chem*. 1990;265:5267–5272.
12. Botelho LH, Rothermel JD, Coombs RV, et al. cAMP analog antagonists of cAMP action. *Methods Enzymol*. 1988;159:159–172.
13. Shimokawa H, Seto M, Katsumata N, et al. Rho-kinase-mediated pathway induces enhanced myosin light chain phosphorylations in a swine model of coronary artery spasm. *Cardiovasc Res*. 1999;43:1029–1039.
14. Uehata M, Ishizaki T, Satoh H, et al. Calcium sensitization of smooth muscle mediated by a Rho-associated protein kinase in hypertension. *Nature*. 1997;389:990–994.
15. Laufs U, Endres M, Stagliano N, et al. Neuroprotection mediated by changes in the endothelial actin cytoskeleton. *J Clin Invest*. 2000;106:15–24.
16. Houghlum K, Lee KS, Chojkier M. Proliferation of hepatic stellate cells is inhibited by phosphorylation of CREB on serine 133. *J Clin Invest*. 1997;99:1322–1328.
17. Kovanecz I, Papp JG, Szekeres L. Long-term ischaemic preconditioning of the heart induced by repeated beta-adrenergic stress. *Acta Physiol Hung*. 1996;84:297–298.
18. Nomura Y, Horimoto H, Mieno S, et al. Repetitive preischemic infusion of phosphodiesterase-III inhibitor olprinone elicits cardioprotective effects in the failing heart after myocardial infarction. *Mol Cell Biochem*. 2003;248:179–184.
19. Clark RB, Friedman J, Dixon RA, et al. Identification of a specific site required for rapid heterologous desensitization of the beta-adrenergic receptor by cAMP-dependent protein kinase. *Mol Pharmacol*. 1989;36:343–348.
20. Strasser RH, Braun-Dullaeus R, Walendzik H, et al. Alpha 1-receptor-independent activation of protein kinase-C in acute myocardial ischemia: mechanisms for sensitization of the adenylyl cyclase system. *Circ Res*. 1992;70:1304–1312.
21. Motomura S, Hagihara A, Narumi Y, et al. Time course of a new ultrashort-acting beta-adrenoceptor-blocking drug, ONO-1101: comparison with those of esmolol and propranolol by using the canine isolated, blood-perfused heart preparations. *J Cardiovasc Pharmacol*. 1998;31:431–440.
22. Sandhu R, Thomas U, Diaz RJ, et al. Effect of ischemic preconditioning of the myocardium on cAMP. *Circ Res*. 1996;78:137–147.
23. Cross HR, Steenberg C, Lefkowitz RJ, et al. Over-expression of the cardiac beta(2)-adrenergic receptor and expression of a beta-adrenergic receptor kinase-1 (betaARK1) inhibitor both increase myocardial contractility but have differential effects on susceptibility to ischemic injury. *Circ Res*. 1999;85:1077–1084.
24. Watanabe Y, Ito M, Kataoka Y, et al. Protein kinase C-catalyzed phosphorylation of an inhibitory phosphoprotein of myosin phosphatase is involved in human platelet secretion. *Blood*. 2001;97:3798–3805.
25. Jo M, Thomas KS, Somlyo AV, et al. Cooperativity between the Ras-ERK and Rho-Rho kinase pathways in urokinase-type plasminogen activator-stimulated cell migration. *J Biol Chem*. 2002;277:12479–12485.
26. Brandt D, Gimona M, Hillmann M, et al. Protein kinase C induces actin reorganization via a Src- and Rho-dependent pathway. *J Biol Chem*. 2002;277:20903–20910.
27. Kitakaze M, Node K, Asanuma H, et al. Protein tyrosine kinase is not involved in the infarct size-limiting effect of ischemic preconditioning in canine hearts. *Circ Res*. 2000;87:303–308.
28. Simonis G, Weinbrenner C, Strasser RH. Ischemic preconditioning promotes a transient, but not sustained translocation of protein kinase-C and sensitization of adenylyl cyclase. *Basic Res Cardiol*. 2003;98:104–113.
29. Utsunomiya T, Satoh S, Ikegaki I, et al. Antianginal effects of hydroxyfasudil, a Rho-kinase inhibitor, in a canine model of effort angina. *Br J Pharmacol*. 2001;134:1724–1730.
30. Endres M, Fink K, Zhu J, et al. Neuroprotective effects of gelsolin during murine stroke. *J Clin Invest*. 1999;103:347–354.
31. Baines CP, Liu GS, Birincioglu M, et al. Ischemic preconditioning depends on interaction between mitochondrial KATP channels and actin cytoskeleton. *Am J Physiol*. 1999;276:H1361–H1368.
32. Terzic A, Kurachi Y. Actin microfilament disrupters enhance K<sub>ATP</sub> channel opening in patches from guinea-pig cardiomyocytes. *J Physiol*. 1996;492(pt 2):395–404.
33. Ledoux S, Laouari D, Essig M, et al. Lovastatin enhances ecto-5'-nucleotidase activity and cell surface expression in endothelial cells: implication of rho-family GTPases. *Circ Res*. 2002;90:420–427.